Drug Design, Development and Therapy

Dovepress
open access to scientific and medical research

Open Access Full Text Article

ORIGINAL RESEARCH

Molecular Mechanism Underlying Effects of Wumeiwan on Steroid-Dependent Asthma: A Network Pharmacology, Molecular Docking, and Experimental Verification Study

Mingsheng Lyu[1,*], Yahui Wang[2,*], Qiuyi Chen[1,*], Jingbo Qin[3], Dan Hou[1], Shuaiyang Huang[1], Dongmei Shao[1], Xuefeng Gong[4], Guirui Huang[1], Shiyu Zhang[1], Zhijie Zhang[1], Hongsheng Cui[1]

[1]Department of Respiratory, The Third Affiliated Hospital, Beijing University of Chinese Medicine, Beijing, People's Republic of China; [2]Department of Neurology and Stroke Center, Dongzhimen Hospital, Beijing University of Chinese Medicine, Beijing, People's Republic of China; [3]National Institute of TCM Constitution and Preventive Medicine, School of Chinese Medicine, Beijing University of Chinese Medicine, Beijing, People's Republic of China; [4]Department of Traditional Chinese Medicine, Beijing Chaoyang Hospital, Capital Medical University, Beijing, People's Republic of China

*These authors contributed equally to this work

Correspondence: Hongsheng Cui, Department of Respiratory, The Third Affiliated Hospital, Beijing University of Chinese Medicine, Beijing, People's Republic of China, Tel +8613901101359, Email hshcui@sina.com

Background: Steroid-dependent asthma (SDA) is characterized by oral corticosteroid (OCS) resistance and dependence. Wumeiwan (WMW) showed potentials in reducing the dose of OCS of SDA patients based on our previous studies.

Methods: Network pharmacology was conducted to explore the molecular mechanism of WMW against SDA with the databases of TCMSP, STRING, etcetera. GO annotation and KEGG functional enrichment analysis were conducted by metascape database. Pymol performed the molecular docking. In the experiment, the OVA-induced plus descending dexamethasone intervention chronic asthmatic rat model was conducted. Lung pathological changes were analyzed by H&E, Masson, and IHC staining. Relative expressions of the gene were performed by real-time PCR.

Results: A total of 102 bioactive ingredients in WMW were identified, as well as 191 common targets were found from 241 predicted targets in WMW and 3539 SDA-related targets. The top five bioactive ingredients were identified as pivotal ingredients, which included quercetin, candletoxin A, palmidin A, kaempferol, and beta-sitosterol. Besides, 35 HUB genes were obtained from the PPI network, namely, *TP53, AKT1, MAPK1, JUN, HSP90AA1, TNF, RELA, IL6, CXCL8, EGFR*, etcetera. GO biological process analysis indicated that HUB genes were related to bacteria, transferase, cell differentiation, and steroid. KEGG pathway enrichment analysis indicated that the potential mechanism might be associated with IL-17 and MAPK signaling pathways. Molecular docking results supported these findings. H&E and Masson staining proved that WMW could reduce airway inflammation and remodeling of model rats, which might be related to the downward expression of IL-8 proved by IHC staining and real-time PCR.

Conclusion: WMW could be a complementary and alternative therapy for SDA by reducing airway inflammation.

Keywords: steroid-dependent asthma, Wumeiwan, Chinese herbal medicine, IL-8, network pharmacology, molecular docking

Introduction

Based on the Global Initiative for Asthma (GINA) (2021 update), steroid-dependent asthma (SDA) is a special phenotype of severe asthma (SA) patients who suffer from frequent exacerbations and/or poor symptoms controlled by high dose inhaled corticosteroid (ICS) - long-acting beta 2-agonist (LABA) of GINA step five treatment and require daily long-term maintenance oral corticosteroid (OCS) treatment as the add-on therapy for the control of asthma to meet the clinical need.[1,2] Frequent and serious exacerbations of SDA lead to shortness of breath, wheezing, chest tightness, and cough, which interfered with daily living and impaired the quality of life of patients. There was no uniform standard for diagnosing SDA in

Received: 18 November 2021
Accepted: 15 February 2022
Published: 30 March 2022

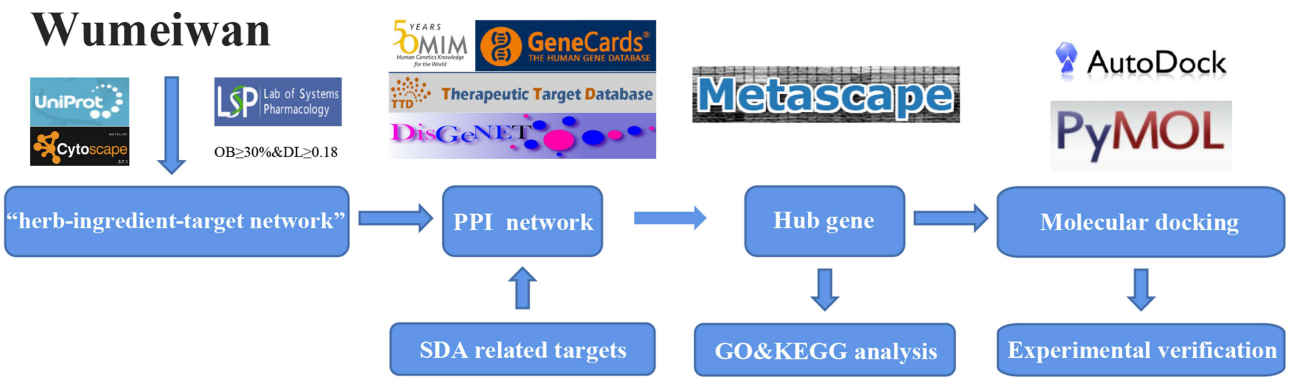

Figure 1 The workflow of the study.

the clinic, but some studies indicated that a dose of five to 40 mg per day of prednisone for three to six months was the necessary criteria.[3,4] Although no large sample epidemiological data of SDA was reported, nearly 20–60% of SA patients had received long-term OCS therapy according to a previous study.[5] However, with the advantage of worldwide easy accessibility, the familiarity of use, and low acquisition costs, long-term exposure to OCS still might induce many side effects including dyspeptic disorders, obesity, infections, diabetes, osteoporosis, and psychiatric disorders.[6] Meanwhile, patients receiving maintenance OCS meet more expensive medical costs than those without maintenance OCS.[7] Although targeted biologics like omalizumab or mepolizumab are recommended for SA patients by GINA as the step five treatment, the application of these medicines is still limited in China for their high medical costs and the long course of treatment.

As an important part of complementary and alternative medicine, Chinese herbal medicine (CHM) is preferred by patients in China because of its few side effects and multi-target therapeutic properties.[8] It was reported that CHM could regulate the immunologic equilibrium mechanism to treat asthma by acting on a number of signaling pathways, such as Notch, JAK-STAT-MAPK, NF-κB, PI3K/AKT, T-bet/Gata-3, and Foxp3-RORγt.[9] Another 13-year population-based retrospective cohort study also showed that CHM might reduce the medical utility of asthmatic patients emergency visits and admissions in hospital, especially for those who used CHM for more than 60 days.[10] Syndrome differentiation and treatment were regarded as the essence of Traditional Chinese Medicine (TCM) theory. Wumeiwan (WMW) is a famous and classical Chinese herbal formula which is first recorded in the "Treatise on Cold Pathogenic and Miscellaneous Diseases" by Zhong-jing Zhang, a famous doctor in the Han Dynasty of ancient China. Given the syndrome of SDA is intermingled heat and cold in TCM theory, with the methods of dispelling cold and clearing heat together, WMW may be classified as the main formula in the TCM treatment of SDA.[11,12] Our previous studies indicated that WMW was a safe herbal medication for SDA individuals, and it could reduce the dose of OCS in SDA patients as well as alleviate patients' clinical symptoms and improve their lung function.[13] Nonetheless, the potential mechanism of WMW against SDA was not fully understood because of its complex compositions and multi-targets.

Network pharmacology establishes a "compound-protein/gene-disease" network and revealing the regulation principles of small molecules in a high-throughput manner, which meets the key idea of the holistic philosophy of TCM and plays a critical role in predicting herb targets, understanding the biological foundation of diseases and syndromes, and identifying disease and syndrome biomarkers.[14–16] In this paper, following the Network Pharmacology Evaluation Method Guidance,[17] network pharmacology and molecular docking were conducted to explore the molecular mechanism of WMW against SDA, then experiments were carried out for verification. The detailed workflow of the study is shown in Figure 1.

Materials and Methods

Components and Bioactive Ingredients in WMW

WMW was composed of *Mume Fructus* ("Wumei" in Chinese, WM), *Coptidis Rhizoma* ("Huanglian" in Chinese, HL), *Phellodendri Chinensis Cortex* ("Huangbo" in Chinese, HB), *Ginseng Radix Et Rhizoma* ("Renshen" in Chinese, RS), *Angelicae Sinensis Radix* ("Danggui" in Chinese, DG), *Cinnamomi Ramulus* ("Guizhi" in Chinese, GZ), *Asari Radix Et*

Rhizoma ("Xixin" in Chinese, XX), *Zingiberis Rhizoma* ("Ganjiang" in Chinese, GJ), *Aconiti Lateralis Radix Praeparata* ("Fuzi" in Chinese, FZ), and *Zanthoxyli Pericarpium* ("Huajiao" in Chinese, HJ). The natural components of WMW were obtained from the traditional Chinese medicine systems pharmacology database (TCMSP, https://old.tcmsp-e.com/index.php, updated on May. 31, 2014), and the bioinformatics analysis tool for the molecular mechanism of traditional Chinese medicine database (BATMAN-TCM, http://bionet.ncpsb.org.cn/batman-tcm, updated on Jan. 2016). They consist of all the 499 Chinese herbs registered in the Pharmacopoeia of the People`s Republic of China (2010 edition),[18,19] from which we could obtain all the information of these components.

Given CHM is usually administered orally in the clinic, oral bioavailability (OB) and drug likeness (DL) are the main screening conditions for medicine absorbing in the gastrointestinal tract. OB refers to the percentage of an orally administered active substance that reaches the systemic circulation, and DL is used to estimate which compounds have similar properties.[20] Therefore, based on previous studies, the criteria of OB≥ 30% and DL≥ 0.18 were used to screen bioactive ingredients from the TCMSP database.[20] For those components obtained from the BATMAN-TCM database, the parameter score≥ 20 and the adjusted *P*-value< 0.05 were necessary for identification.[20]

Targets Related to Bioactive Ingredients

Targets related to bioactive ingredients in WMW were obtained from the TCMSP database and the BATMAN-TCM database. These two databases adopted complicated methods: (1) For those drug-target interactions validated by experiment, targets information were retrieved from databases such as Herb Ingredients` Targets.[21] (2) For those compounds without validated targets, a similarity-based target prediction based on the known drug-target interactions method was used to do the prediction.[18,19] Since the targets might be incomplete, the Swiss Target Prediction web service was also used to get more accurate predicted targets of WMW by using the 2-dimensional (2D) structure of bioactive ingredients obtained from PubChem. Relevant parameters of Swiss Target Prediction were set included the organism for "*Homo sapiens*" and the probability≥ 0.6.[22] Finally, standardized the gene names of targets related to bioactive ingredients with the species limited into "*Homo sapiens*" by UniProt Knowledgebase (UniProtKB, http://www.uniprot.org, updated on Jan. 28, 2021).

SDA-Related Targets and Common Targets Between WMW and SDA

It could obtain more targets relevant to SDA by searching databases as many as possible. Targets were collected from GeneCards the human gene database (https://www.genecards.org, updated on Apr. 28, 2021),[23] Online Mendelian Inheritance in Man database (OMIM, http://www.omim.org, updated on Apr. 30, 2021),[24] Therapeutic Target Database (TTD, http://db.idrblab.net/ttd, updated on Jun. 1, 2020),[25] and DisGeNET database (http://disgenet.org, updated on May. 4, 2021)[26] by using the keywords of "steroid-dependent asthma" and/or "corticosteroid-dependent asthma". After removing the repetitive targets retrieved from various databases, the target database of SDA was built. They were also standardized in the UniProtKB database. The potential effecting targets of WMW against SDA were screened by comparing the common targets between SDA-related targets and the predicted targets of WMW. With these common targets, the "herb-ingredient-target" network was created by Cytoscape software (version 3.7.1) (http://www.cytoscape.org).[27] To identify the pivotal ingredients of WMW, "Network analysis" tool in Cytoscape was used to get the "degree (DC)" information of bioactive ingredients from the "herb-ingredient-target" network.

Construction of the Protein–Protein Interaction Network

Search Tool for the Retrieval of Interacting Genes/Proteins (STRING, https://string-db.org/, updated on Oct. 17, 2020) is a database of known and predicted protein-protein interactions (PPI), which are ultimately essential for implementing a functional system.[28] The following parameters of STRING were set including the organism for "*Homo sapiens*" and the minimum required interaction score≥ 0.9. Given the PPI network was complex, we conducted the topology analysis of the PPI network to get HUB genes by means of Cytoscape. Specifically, the parameter information of "DC", "betweenness centrality (BC)", "closeness centrality (CC)", and "stress" was obtained by "Network analysis" tool of Cytoscape. If the DC of a node was more than twofold the median degree of all the nodes in the network, meanwhile BC, CC, and stress were higher than the corresponding median values of their own, the node might function as a HUB gene.[29] At last, visual processing was made by Cytoscape.

Gene Ontology and KEGG Pathway Enrichment Analysis

Metascape (http://www.metascape.org, updated on May. 1, 2021) database was used for pathway enrichment analysis, which could provide a comprehensive gene list annotation and analysis resource.[30] In order to obtain the biological processes and relevant targets of HUB genes, biological processes (BPs), cell components (CCs), and molecular functions (MFs) of Gene Ontology (GO) annotation and Kyoto Encyclopedia of Genes and Genomes (KEGG) functional enrichment analysis were conducted by metascape database with a considering significant P-value ≤ 0.05.

Molecular Docking

AutoDock (version 4.2.6) (http://www.autodock.scripps.edu, updated on Feb. 27, 2013) was used to predict how bioactive ingredients bind to HUB genes with the 3D structure.[31] Usually, the former one was called ligands as well as receptor proteins for the latter one. The top 10 genes were selected as the core target receptor proteins after sorted the DC value of HUB genes by size. The structures of receptor proteins were obtained from the RCSB Protein Data Bank database (PDB, https://www.rcsb.org, updated on Apr. 27, 2021),[32] and that of ligands were downloaded from TCMSP. After deleting water and adding hydrogen of ligands and receptor proteins, molecules were converted from pdb or mol2 to pdbqt, and molecular docking was performed by AutoDock. The binding energy of less than 0 kcal/mol indicates that the conformation of ligands and receptor proteins can be stably bound; the larger the absolute value, the stronger the stability.[20] Visualization of receptor protein-ligand interactions was performed by open source Pymol (version 2.4) (https://pymol.org/, updated on Jun. 2, 2020).

Animals

To verify the predicted target, we conducted an animal experiment. Male Sprague Dawley rats were purchased from SBF (Beijing) Biotechnology Co., Ltd (Beijing, China), weighted 120–140 g with four-five weeks of age. The rats were bred in the school of basic medicine of Beijing University of Chinese Medicine[certification SCXK (Jing) 2016-0002]. Rats were housed in a room with a temperature of 22±2°C, a humidity of 55±5%, and a 12 hours light-controlled environment. Animals were raised with accessing food and water freely and allowed to acclimatize themselves for one week before the initiation of the experiment. This study was approved by the Research Ethics Committee of Beijing University of Chinese medicine[No. BUCM-4-2018031001-1012] and followed the laboratory animal guideline for ethical review of animal welfare[GB/T 35892-2018].

Drug and Reagents

Ovalbumin (OVA) was purchased from sigma Co., Ltd. (Louis, MO, USA)[A5378-1G]. Imject™ Alum Adjuvant, which contains aluminum hydroxide (40mg/mL) and magnesium hydroxide (40mg/mL), was purchased from Thermo Fisher Scientific (Waltham, MA, USA)[77161]. Dexamethasone sodium phosphate injection (DEX) was brought from Sinopharm Rongsheng Pharmaceutical Co., Ltd. (Henan, China)[H41020036]. Modified Masson trichrome stain was purchased from Beijing Solarbio Science & Technology Co., Ltd (Beijing, China)[G1345]. Rabbit Anti-IL-8/CXCL8 antibody was purchased from Bioss Antibodies (Beijing, China)[bs-0780R]. Peroxidase-conjugated goat anti-rabbit IgG (secondary antibody) and 3,3`-diaminobenzidine (DAB) were purchased from ZSGB-BIO (Beijing, China)[PV-9001 and ZLI-9018]. RaPure Total RNA Mini Kit was brought from Guangzhou Magen Biotechnology Co., Ltd. (Guangzhou, China)[R4011-03]. All-in-One First-Strand Synthesis Master Mix was brought from Fujian BioMED Medical Technology Co., Ltd (Fujian, China) [BM60501S]. 2x qPCR SYBR Green Master Mix was brought from Dalian Meilunbio Biotechnology Co., Ltd (Dalian, China)[MA0691-1]. Primers were synthesized by Sangon Biotech (Shanghai, China). Compression atomizer (Omron Health Care China Co., Ltd)[NE-C900] were employed for the OVA challenge. Stratagene Mx3000P (Stratagene, La Jolla, CA) was used for fluorescence quantitation. Olympus BX-60 upright microscope (Tokyo, Japan) performed image acquisition.

All herbal granules of WMW formula were purchased from Good Manufacturing Practice (GMP)-certified pharmaceutical company, Beijing Tcmages Pharmaceutical Co., Ltd. Specifically, the dosage of the granule was converted from WMW formula pieces: WM 10g, HL 6g, HB 6g, *RS* 10g, DG 10g, GZ 6g, XX 3g, GJ 3g, FZ 10g, and HJ 10g. The daily

dose of WMW formula was processed into 18g granules. At last, granules were dissolved in 400 mL water at a temperature of 100°C and stored at 4°C after it cools.

OVA-Induced Plus Descending DEX Intervention Chronic Asthmatic Model and Therapeutic Interventions

Given SDA belonged to chronic asthma or SA with long-term courses, we built the OVA-induced plus descending DEX intervention chronic asthma (OVA+DEX) model based on our previous studies.[33] Rats were equally and randomly divided into four groups: control group, OVA-induced chronic asthma (OVA) group, OVA+DEX group, and WMW group. Each group contained three rats. The rats in the OVA group, OVA+DEX group, and WMW group were intraperitoneally injected with a 1.0 mL saline mixture containing 100mg OVA and 100mg aluminum hydroxide on day 1 and day 8 for sensitization. The control group was intraperitoneally injected with the same amount of saline. From day 15, all rats except the control group were challenged with 1% OVA nebulization inhalant solution every two days at the rate of 0.25mL/min for 30 minutes, and it would last for seven weeks, while the control group inhaled the same amount of saline. To simulate the descent use of glucocorticoid from a high-dose to a low-dose of SDA patients, we adopted a method of descending glucocorticoid administration for rats. Specifically, OVA+DEX group and WMW group rats were intraperitoneally injected with 0.5mg/kg DEX 30 minutes before the OVA challenge from day 15 to day 28. Then DEX was withdrawn at the rate of 0.1mg/kg per week from day 29 to the end of the challenge.[33] The OVA group and control group were injected with the same amount of saline from day 15 to the end. Besides, rats in the WMW group were administered WMW formula granules with the dose of 1.86g/kg through gastric administration at 30 minutes before the OVA challenge once a day from day 15 to the end (the dosage of WMW formula granules is determined based on the results of pre-experiment, which is not described in this paper). All rats were sacrificed on day 63. The sensitization, challenge, and therapeutic interventions were shown in Figure 2.

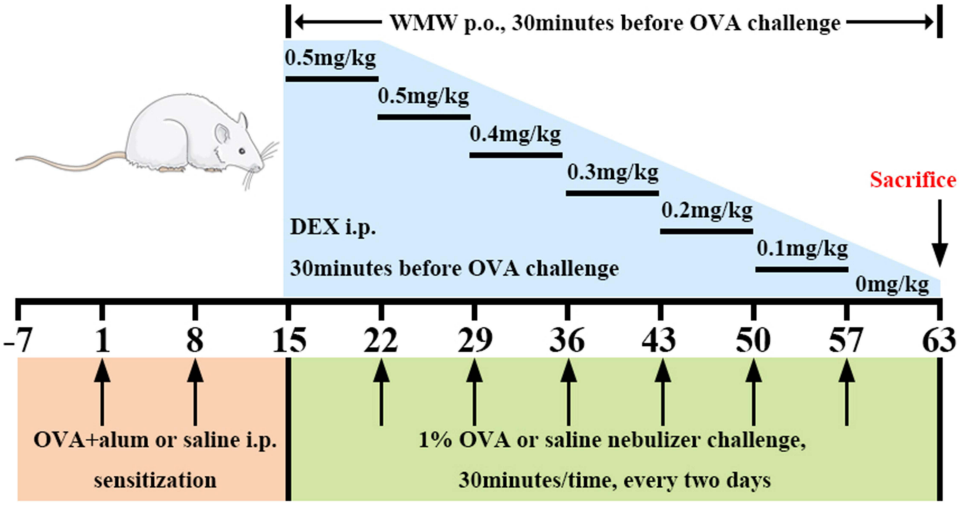

Group	Sensitization	Challenge	Intervention
Control	Saline	Saline	Saline
OVA	OVA+alum	1%OVA	Saline
OVA+DEX	OVA+alum	1%OVA	DEX
WMW	OVA+alum	1%OVA	DEX+WMW

Figure 2 Schematic diagram of OVA-induced plus descending DEX intervention chronic asthmatic model. Sensitization: the mixture of OVA and aluminum hydroxide was intraperitoneally injected into rats at day 1 and 8. Challenge: from day 15, rats were challenged with 1% OVA nebulization inhalant solution every two days for 30 minutes, and it would last for seven weeks. Therapeutic interventions: DEX was intraperitoneally injected into rats with the dosage of 0.5mg/kg in day 15 to day 28, and it was withdrawn at the rate of 0.1mg/kg per week from day 29 to the end of the challenge.

Lung Histopathology and Immunohistochemistry

Lung tissues were fixed overnight in 4% paraformaldehyde solution, dehydrated and embedded in paraffin. Tissue sections (4 μm) were made, and dyed with hematoxylin/eosin (H&E) and Masson staining following the standard manufacturer's protocol. The inflammatory degree was scored based on the H&E staining by two independent observers who were blinded to the experiment. Briefly, grades of 0 to 4 were given based on a previous study: score 0 for no inflammation, score 1 for occasional cuffing with inflammatory cells, score 2 for most bronchi or vessels were surrounded with inflammatory cells by a thin layer, and score 3 and 4 for a moderate layer and a thick layer respectively.[34] Immunohistochemistry (IHC) was conducted to identify the positive expression of IL-8 around the airway epithelial cells. Detailed steps of IHC staining were as follows:[35] sections were boiled bathing with citrate buffer (pH 6.0) for 15min, then they were washed in phosphate-buffered saline before blocking endogenous peroxidase with 3% hydrogen peroxide for 30min. Then normal goat serum was used to block non-specific binding of the antibodies at 37°C for 20 min, after which sections were incubated overnight at 4°C with IL-8 primary antibodies (1:500). Sections were incubated with secondary antibodies for 20 min after incubation with primary antibodies. Finally, sections were stained and developed with DAB. After nuclear staining with hematoxylin, the stained sections were observed under a microscope at 400× magnification (Olympus BX60, Tokyo, Japan). ImageJ software (version 1.53, National Institutes of Health) performed the image quantitative analysis. Simply, the brown stained area on IHC staining was separated with the method of auto threshold in ImageJ after the image was converted into RGB stack type, then the average optical density (AOD) of each image was measured and calculated to assess IL-8 staining strength. Similar steps were applied to Masson staining. The collagen volume fraction of Masson staining images reflected the percentage area (% Area) of the total surface occupied by the blue-stained collagen area.

Real-Time Quantitative Polymerase Chain Reaction (Real-Time PCR)

Total RNA was extracted and purified from the upper left lung of each group of rats using RaPure Total RNA Mini Kit according to the manufacturer's instructions. Then total RNA was reverse transcribed to cDNA using All-in-One First-Strand Synthesis Master Mix. Real-time PCR was performed using a Stratagene Mx3000P as follows: the reaction mixture consisted of 10 ul 2x qPCR SYBR Green Master Mix, 10 μM forward and reverse primer, 2 ul cDNA, and the final volume of the mixture was adjusted to 20 μL with the addition of nuclease-free water. The cDNA was amplified at 95°C for 60s, followed by 45 cycles of PCRs: at 95°C for 10s, at 60°C for 30s, successively. Detailed primers were in the following: CATTAATATTTAACGATGTGGATGCGTTTCA (IL-8 forward), GCCTACCATCTTTAAACTGCACAAT (IL-8 reverse), TATGCTCTCCCTCACGCCATCC (β-actin forward), GTCACGCACGATTTCCCTCTCAG (β-actin reverse). The relative expressions of the gene was calculated using the $2^{-\Delta\Delta Ct}$ method.

Data Analysis and Statistics

SPSS 20.0 statistical software (SPSS Inc., USA) performed the statistical analysis. All data were expressed as Mean ± SEM (standard error of the mean). One-way analysis of variance (ANOVA)/ post hoc least-significant difference (LSD) test and nonparametric test were respectively used to compare the unpaired parametric or nonparametric data between groups. The *P*-value of less than 0.05 was considered statistically significant.

Results

Bioactive Ingredients and Predicted Targets in WMW

With the criteria mentioned above (OB ≥ 30% and DL ≥ 0.18 for TCMSP; the parameter score ≥ 20 and the adjusted *P*-value < 0.05 for BATMAN-TCM), a total of 129 bioactive ingredients were identified in WMW, of which 8 were from WM, 14 were from HL, 37 were from HB, 22 were from RS, 2 were from DG, 7 were from GZ, 8 were from XX, 5 were from GJ, 21 were from FZ, and 5 were from HJ. After removing repetitive ingredients, 102 bioactive ingredients were left. Detailed information was listed in Supplementary Table 1.

Targets of 102 bioactive ingredients in WMW were predicted by TCMSP database, the BATMAN-TCM database, and Swiss Target Prediction. Respectively, 192, 184, 210, 118, 54, 53, 110, 46, 21, and 174 potential target genes were predicted for WM, HL, HB, RS, DG, GZ, XX, GJ, FZ, and HJ. After removing repetitive targets, 241 genes were obtained.

SDA-Related Targets and Common Targets Between WMW and SDA

By screening GeneCards, OMIM, and DisGeNET database, 3539 SDA-related targets were obtained. By comparing the targets of WMW and SDA, 191 common targets from SDA were shared with those of the bioactive ingredients of WMW (Supplementary Table 2). Based on the above data, the "herb-ingredient-target" network was made by Cytoscape and shown in Figure 3, which comprised 294 nodes and 1755 edges. Each edge represents the relationship between herb ingredients and target genes, the closer the nodes are connected, the larger the area of the node is. Besides, the following top five pivotal ingredients were identified with the method mentioned above: quercetin (MOL000098), candletoxin A (MOL002671), palmidin A (MOL000762), kaempferol (MOL000422), and beta-sitosterol (MOL000358). Jvenn plug-in performed the common targets network (Figure 4).[36]

PPI Network Construction and HUB Gene Screening

PPI network analysis on common targets was performed by STRING database, and it was shown in Figure 5A. With 191 nodes, 773 edges, and an average node degree of 8.09, the PPI network performed the interaction of common targets and depicted the biological processes of WMW against SDA. Based on the four parameters of "DC", "BC", "CC" and "stress", "Network analysis" tool in Cytoscape was used to conduct the topology analysis and obtain the HUB genes of WMW. The median degree of DC, BC, CC, and stress was seven, 0.340164, 0.002839, and 654. Finally, 35 HUB genes

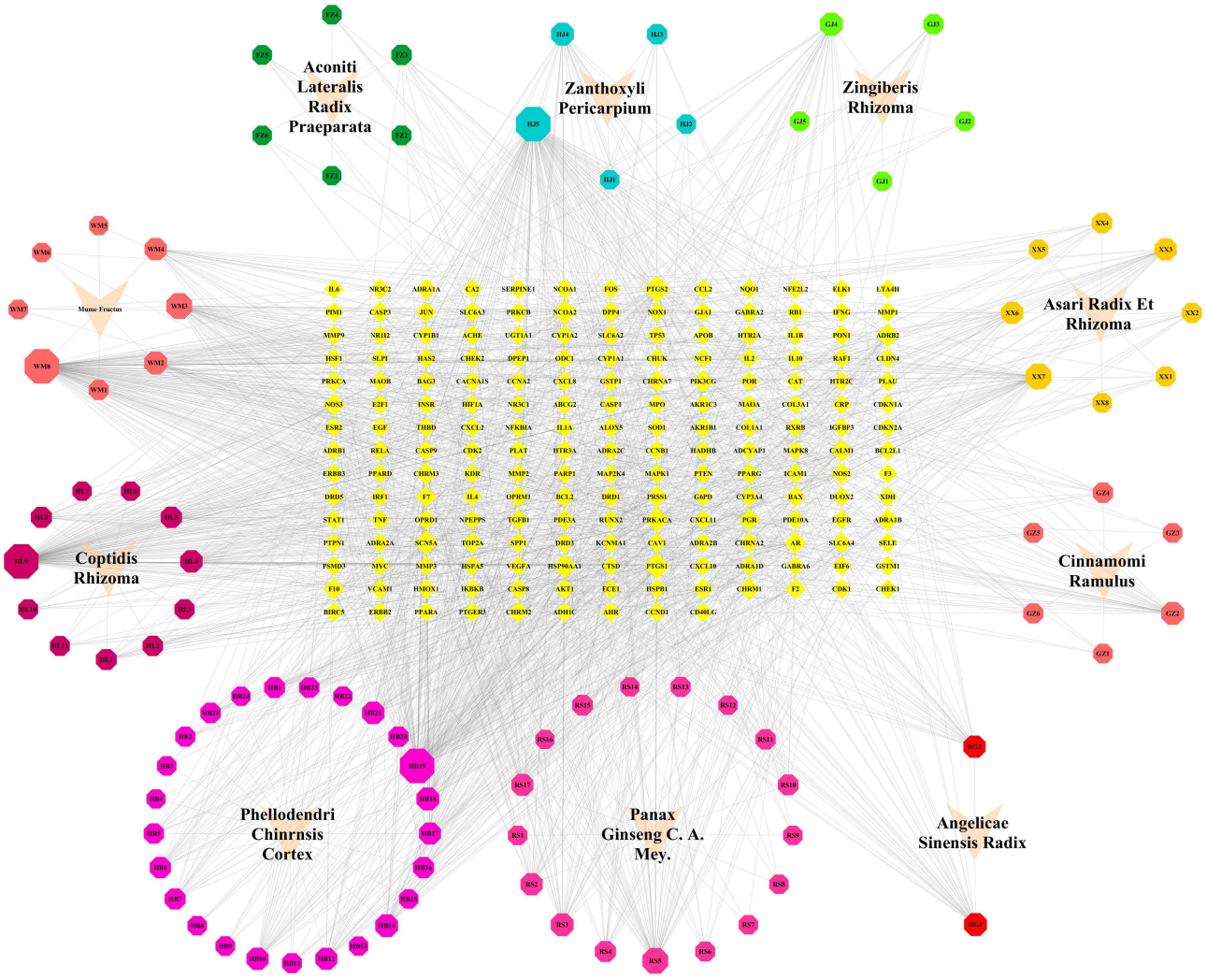

Figure 3 The "herb-ingredient-target" network. The inverted triangle, octagon, and diamond corresponded to the herb, ingredient, and target respectively. The closer the nodes were connected, the larger the area of the node was.

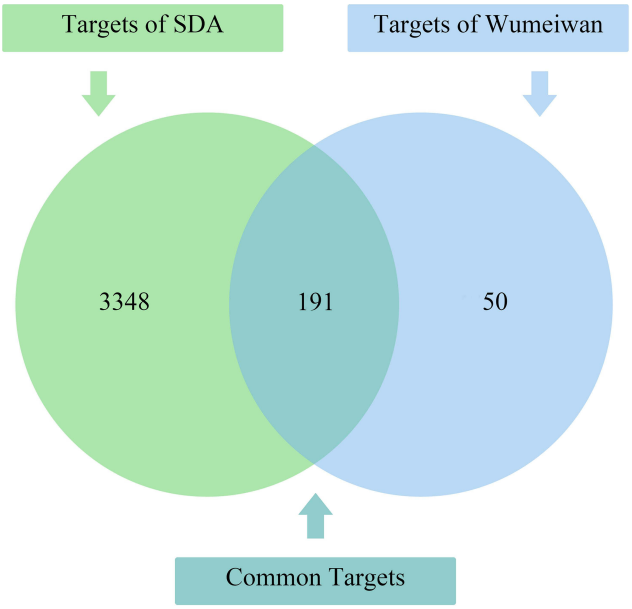

Figure 4 Venn diagram of common targets.

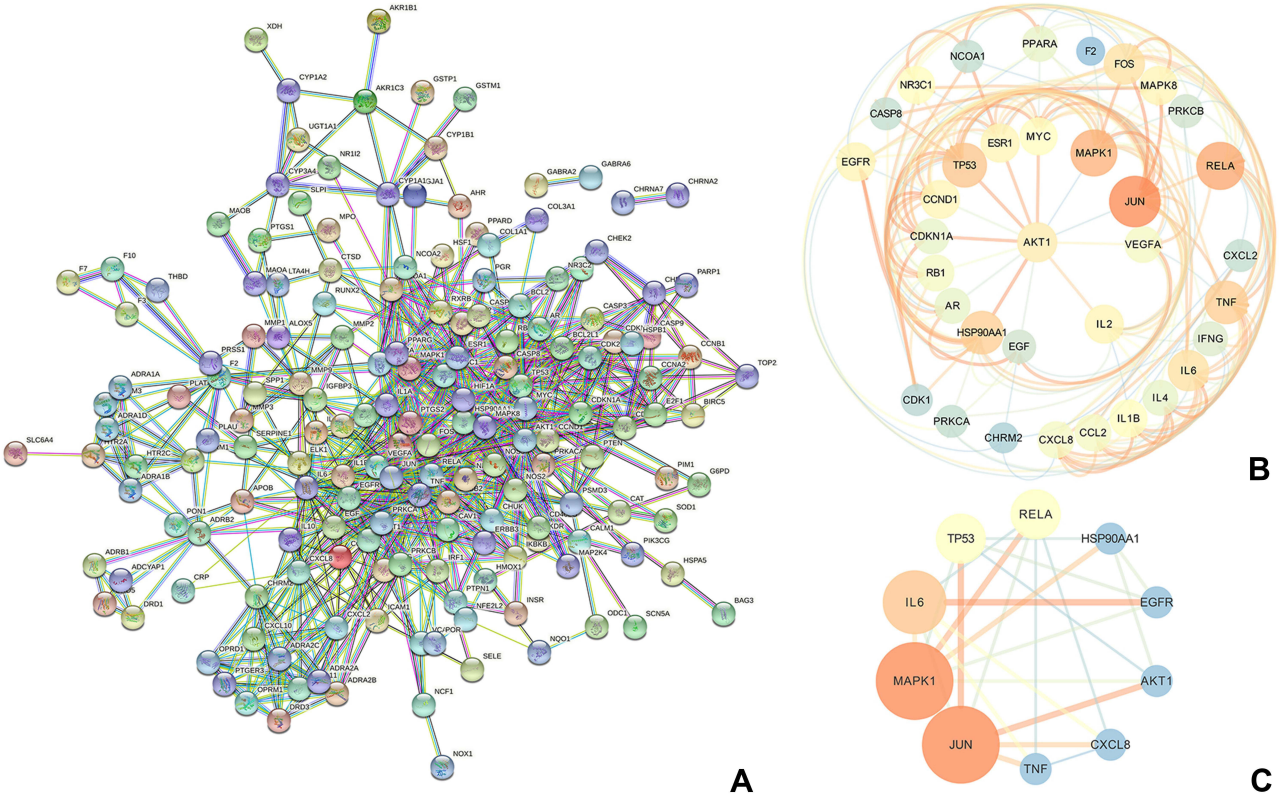

Figure 5 Screening of HUB genes. (**A**) PPI network of WMW against SDA performed by STRING database with the parameters of the organism for "*Homo sapiens*" and the minimum required interaction score≥ 0.9. (**B**) 35 HUB genes network performed by Cytoscape yFiles Radial Layout. Low degree values showed large sizes and bright colors, and small sizes and dark colors for high degree values on the contrary. (**C**) The 10 core targets network, including *JUN, MAPK1, IL6, TP53, RELA, HSP90AA1, EGFR, AKT1, CXCL8*, and *TNF*.

were obtained after screening data (Table 1). Cytoscape performed the visual processing of HUB genes, with the setting of large sizes and bright colors for low degree values, and small sizes and dark colors for high degree values on the contrary (Figure 5B). Sorted DC values by size, the 10 core targets were identified, and the network was shown in Figure 5C.

GO Function and KEGG Pathway Analysis

Metascape database was used to analyze the BPs, CCs, and MFs of the GO function and KEGG pathways on 35 HUB genes. 595 BPs, 22 CCs, 58 MFs, and 260 KEGG pathways related to SDA were obtained with the criteria of the *P*-value<0.01, a minimum count of 3, and an enrichment factor> 1.5. Similar terms were enriched to one representative cluster, and the top 10 significantly enriched clusters in BPs, CCs, and MFs were selected for analysis, as well as top 20 significant KEGG pathways were enriched. It was shown in Figures 6 and 7 by Hiplot (https://hiplot.com.cn), a comprehensive web platform for scientific data visualization. BPs enrichment analysis demonstrated that the HUB genes were related to bacteria, transferase, cell differentiation, and steroid. The main MFs of HUB genes were cytokine

Table 1 DC, BC, CC, and Stress Information of HUB Genes

Number	Hub Gene Name	Degree	Betweenness Centrality	Closeness Centrality	Stress
1	TP53	37	0.08694128	0.45355191	16624
2	AKT1	36	0.08522859	0.44504021	15118
3	MAPK1	36	0.12742872	0.49112426	20616
4	JUN	36	0.09645964	0.48538012	19138
5	HSP90AA1	33	0.1062704	0.46368715	16540
6	TNF	33	0.05921156	0.45730028	9786
7	RELA	32	0.04454007	0.45604396	10492
8	IL6	25	0.03953757	0.42783505	7584
9	CXCL8	24	0.04595284	0.40389294	8538
10	EGFR	23	0.06353801	0.44864865	10124
11	FOS	22	0.02112597	0.43569554	5042
12	ESR1	21	0.02791165	0.4403183	5578
13	MAPK8	21	0.01921663	0.41708543	4802
14	VEGFA	20	0.02932016	0.43684211	5530
15	RB1	19	0.02473773	0.42025316	5420
16	PRKCA	18	0.03881227	0.41708543	7520
17	MYC	18	0.01938051	0.41919192	3630
18	NR3C1	18	0.01061043	0.41813602	3170
19	F2	17	0.11206153	0.38694639	15498
20	PRKCB	17	0.0229569	0.40096618	5236
21	CCND1	17	0.01260435	0.40487805	3530
22	CDKN1A	17	0.00883462	0.39808153	2578
23	IL1B	17	0.00915936	0.39712919	2126
24	CXCL2	16	0.00700863	0.35394456	1818
25	EGF	16	0.02763723	0.41089109	4252
26	CHRM2	15	0.02079833	0.36165577	2596
27	IL4	15	0.04035183	0.39243499	5480
28	CASP8	15	0.02310684	0.39150943	4716
29	NCOA1	15	0.03587812	0.38785047	9074
30	IL2	14	0.00681991	0.41919192	1898
31	AR	14	0.00890765	0.38248848	2636
32	CDK1	14	0.011109	0.35853132	3066
33	CCL2	14	0.00497893	0.38694639	1498
34	IFNG	14	0.01205977	0.39712919	2862
35	PPARA	14	0.08271518	0.44266667	14568

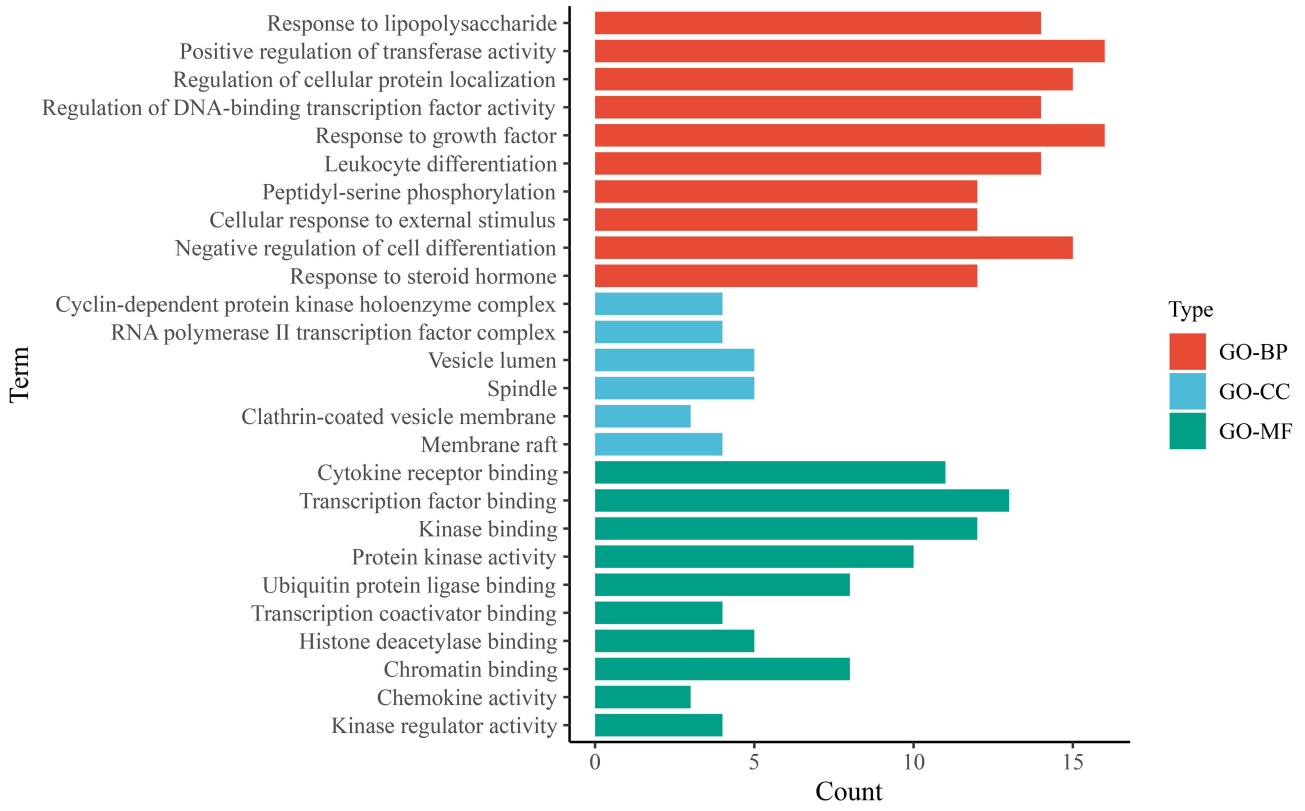

Figure 6 GO function of HUB genes. The horizontal axis represented the counts of genes in the enriched terms, and the vertical axis represented the specific terms of BPs, CCs, and MFs.

receptor binding, transcription factor binding, and kinase binding. The CCs of HUB genes were enriched in cyclin-dependent protein kinase, RNA polymerase II, and vesicle lumen. From the results of KEGG pathways analysis, it was indicated that the potential mechanism of WMW against SDA might be associated with IL-17 signaling pathway, human cytomegalovirus infection, AGE-RAGE signaling pathway, MAPK signaling pathway, PI3K-Akt signaling pathway, TNF signaling pathway, endocrine resistance, etcetera.

Molecular Docking

The 10 core target receptor proteins and five pivotal ingredients were used to finish the molecular docking. Detailed information of docking results was listed in Table 2 and Figure 8. The binding energy of less than −5 kcal/mol indicates a stronger connection of ligands and receptor proteins.[37] Hence, we screened out the receptor protein-ligand interactions with the lowest energy, which was CXCL8, and it was visualized by Pymol (Figure 9). These results indicated that potential pivotal ingredients of WMW had excellent abilities to spontaneously bind the receptor proteins of SDA.

WMW Decreased the Airway Inflammation and Airway Remodeling in Lung Tissues

In order to evaluate the model and detect the effects of WMW on airway inflammation and airway remodeling, H&E and Masson staining were observed. The results of the H&E staining inflammatory degree showed that OVA group and OVA +DEX group rats showed significant inflammatory cell infiltration and airway epithelial thickening in the peribronchial and perivascular regions, while it was not observed in the control group ($P<0.05$). Compared with the OVA group, inflammatory cell infiltration in the WMW group was significantly reduced ($P<0.05$), but it was still obviously shown in the OVA+DEX group ($P>0.05$) (Figure 10A and D).

Results of Masson staining showed that the collagen deposition around the airway increased gradually and significantly in the OVA group and the OVA+DEX group ($P<0.01$), which indicated the gradual progression of airway

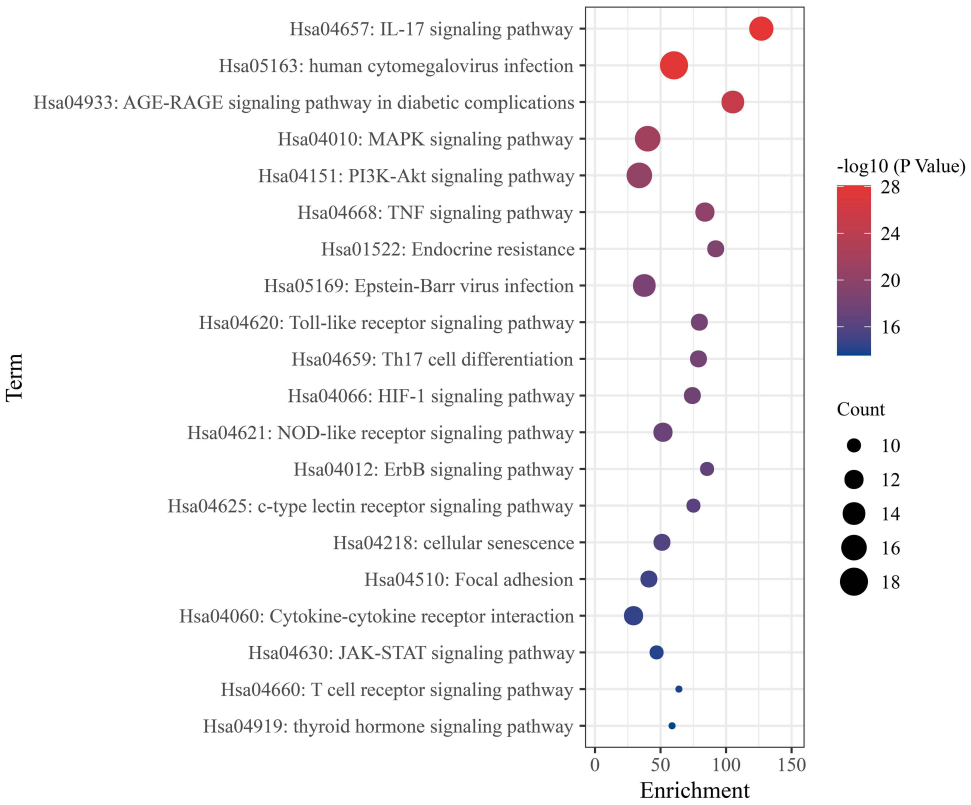

Figure 7 KEGG pathway analysis. Bubble plot performed the top 20 signaling pathways of WMW against SDA. The horizontal axis represented the enrichment scores of pathways, and the vertical axis represented the names of pathways. The counts of genes in each enriched pathway were presented via the bubble, and the *P*-value was marked by the bubble color.

remodeling. Interestingly, the OVA+DEX group showed similar pathological changes as the OVA group instead of as normal as we predicted before, and there was no statistical difference in collagen volume fractions between the OVA group and the OVA+DEX group (P=0.548). On the contrary, compared with these two groups, collagen deposition was found to be attenuated by treating with WMW (P<0.01) (Figure 10B and E).

WMW Inhibited the Expression of IL-8 in the Lung of OVA-Induced Plus Descending DEX Intervention Chronic Asthmatic Model

CXCL8 is the transcriptional gene of IL-8. Results from molecular docking indicated CXCL8 had the lowest receptor protein-ligand interactions energy. Hence, we conducted the IHC staining and real-time PCR of IL-8 for further verifications. It was shown in the IHC staining that the expression of IL-8 was significantly increased in the OVA group and OVA+DEX group comparing with the control group (P<0.01), but there was no statistical difference between these two groups (P=0.053). While the expression of IL-8 was significantly decreased in the WMW group comparing with the OVA group and OVA+DEX group (P<0.01), which suggested WMW might reduce the airway inflammation by inhibiting the secretion of IL-8 (Figure 10C and F). As a result of analyzing IL-8 gene expression using real-time PCR, similar findings were observed. As shown in Figure 10G and Table 3, the relative expression of IL-8 in the OVA group and OVA+DEX group were significantly increased respectively when compared to the control group (P<0.01), and WMW decreased these abnormalities (P<0.05). The statistical difference in relative expression of IL-8 was not found between the OVA group and OVA+DEX group (P=0.07).

Discussion

SDA is a special phenotype of SA characterized by OCS dependence. Despite OCS is the second-line therapy for step five treatment asthmatic patients recommended by GINA, 40% of them still receive regular OCS at a daily dose of

Table 2 Molecular Docking Results

Ligands	Receptor Proteins	PDB Entry	Binding Energy (kcal/mol)
Quercetin	TP53	2X0W	−5.9
	AKT1	1UNR	−5.34
	MAPK1	6SLG	−4.08
	JUN	5T01	−4.63
	HSP90AA1	3T10	−5.09
	TNF	5UUI	−5.42
	RELA	4KV1	−4.54
	IL6	1ALU	−4.89
	CXCL8	4XDX	−7.24
	EGFR	5UG9	−4.41
Candletoxin A	TP53	2X0W	−3.96
	AKT1	1UNR	−4.9
	MAPK1	6SLG	−4.01
	JUN	5T01	−2.65
	HSP90AA1	3T10	−5.25
	TNF	5UUI	−6.71
	RELA	4KV1	−5.64
	IL6	1ALU	−5.12
	CXCL8	4XDX	−10.07
	EGFR	5UG9	−7.26
Palmidin A	TP53	2X0W	−6.19
	AKT1	1UNR	−5.34
	MAPK1	6SLG	−4.79
	JUN	5T01	−4.79
	HSP90AA1	3T10	−5.8
	TNF	5UUI	−8.15
	RELA	4KV1	−6.67
	IL6	1ALU	−7.21
	CXCL8	4XDX	−9.87
	EGFR	5UG9	−6.73

(*Continued*)

Table 2 (Continued).

Ligands	Receptor Proteins	PDB Entry	Binding Energy (kcal/mol)
Kaempferol	TP53	2X0W	−6.71
	AKT1	1UNR	−5.45
	MAPK1	6SLG	−5.21
	JUN	5T01	−5.94
	HSP90AA1	3T10	−6.22
	TNF	5UUI	−6.28
	RELA	4KV1	−6.09
	IL6	1ALU	−6.15
	CXCL8	4XDX	−8.86
	EGFR	5UG9	−6.77
Beta-sitosterol	TP53	2X0W	−5.4
	AKT1	1UNR	−6.47
	MAPK1	6SLG	−7.51
	JUN	5T01	−9.31
	HSP90AA1	3T10	−8.88
	TNF	5UUI	−7.47
	RELA	4KV1	−7.08
	IL6	1ALU	−5.51
	CXCL8	4XDX	−10.2
	EGFR	5UG9	−7.25

15mg.[38] Usually, the phenotypes of asthma are classified into type 2-high asthma and type 2-low asthma. The former is associated with type 2 helper T(Th2) cells responses, while the latter is associated with obesity, aging, and smoking.[39] Conventional wisdom would seem to suggest SDA belongs to type 2-high asthma,[40] but recent studies supposed that the airway inflammation in SA is not limited to Th2 cells responses and eosinophilic inflammation. Transcriptomic and proteomic analysis from SA cohorts recruited in the Unbiased Biomarkers for the Prediction of Respiratory Diseases Outcomes (U-BIOPRED) study indicated that mixed neutrophilic/eosinophilic inflammation was more prevalent in patients with SA compared with mild/moderate asthma,[41] which meant more individualized treatment was needed in SDA.

The pathogenesis of SDA is complex, the potential mechanisms include the following parts:[1] (1) Activation of the p38 MAPK pathway lead to decreased affinities of the phosphorylated glucocorticoid receptor (GR) to corticosteroids; (2) Increased expression of GRβ compete with GRα to bind corticosteroids; (3) Interaction between GRs via coactivator molecules and inflammatory transcription factors NF-κB may not be efficient; (4) Histone acetylation is defective. Finally, corticosteroid resistance and dependence are induced, and unsatisfied curative effects of OCS occur in SDA individuals. Since the introduction of biological agents, treatment strategies of SDA have been drastically changed. Although monoclonal antibodies have the effects of inhibiting the migration of eosinophils to airways or decreasing the free immunoglobulin E (IgE) to decrease the OCS requirement in SA patients, meanwhile avoiding the side effects of

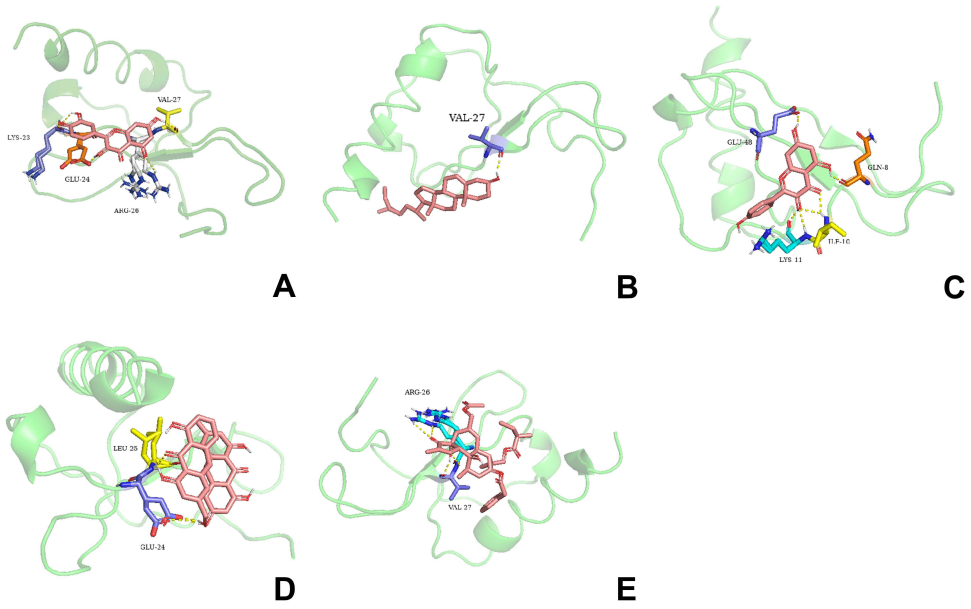

Figure 8 Molecular docking between CXCL8 and five pivotal ingredients, including quercetin (**A**), beta-sitosterol (**B**), kaempferol (**C**), palmidin A (**D**), and candletoxin A (**E**).

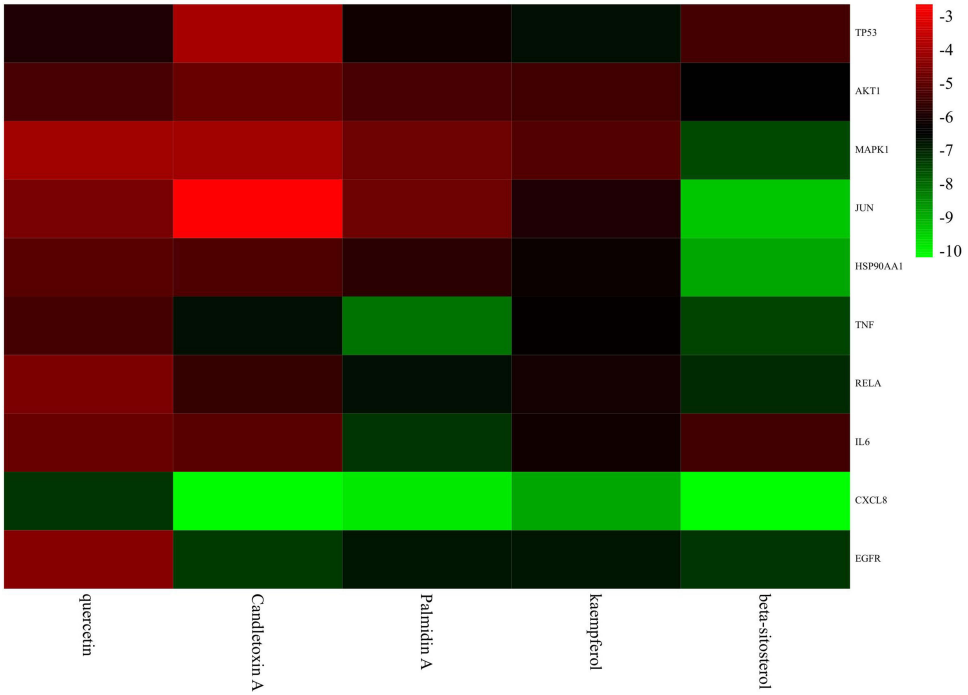

Figure 9 Correlation heatmap of docking results between the 10 core targets and five pivotal ingredients. The binding energy was marked by different colors, red for higher scores and green for lower scores. It could be observed that all core targets could stably bind with five pivotal ingredients, especially CXCL8 showed the lowest energy.

OCS, there are just a few biologics are approved for type 2-high asthma and have the potential to be used for SDA, such as mepolizumab (anti-IL5), benralizumab (anti-IL5R), and dupilumab (anti-IL4Rα).[40] Even so, the application of biologics is limited in China for their high medical costs and the long course of treatment.

TCM has been used in Asian countries for thousands of years, and it has been spread to 183 countries and regions. As a classical formula of TCM, WMW showed potential treatment prospects in the field of chronic colitis, obesity, diabetes,

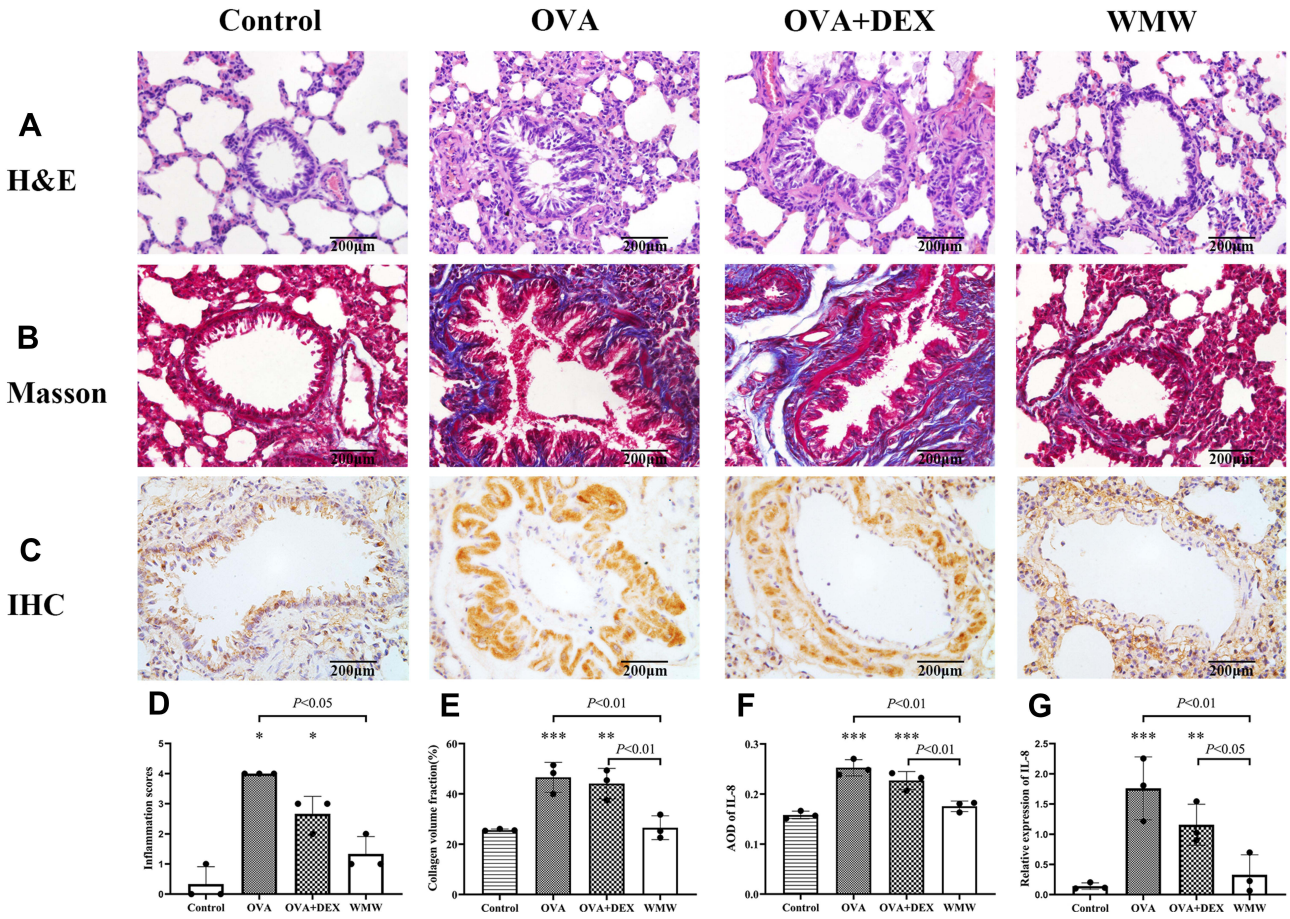

Figure 10 Effects of WMW on pathological features of OVA-induced plus descending DEX intervention chronic asthmatic model. WMW treatment could reduce the airway inflammations ((**A**) H&E staining, magnification×400, (**D**) inflammation scores), airway remodeling ((**B**) Masson staining, magnification×400, (**E**) calculations of collagen volume fraction), and the expression of IL-8 ((**C**) IHC staining, magnification×400, (**F**) IL-8 average optical density of IHC staining images, (**G**) Relative expressions of IL-8 performed by real-time PCR) in model rats. All results were expressed as Mean ± SEM. Compared with the control group, **P*<0.05, ***P*<0.01, ****P*<0.001.

and ulcerative colitis.[42–45] Based on the components of WMW, researchers created Food Allergy Herbal Formula, which was the first botanical investigational new drug approved for clinical studies for food allergy by the US Food and Drug Administration.[46] Given that OCS had lots of side effects, reducing the dose of OCS was categorized as one of the hot topics for the academics. Our previous studies showed that WMW could help to reduce the dose of OCS in SDA patients,[13] while the specific mechanism was not clear. Hence, we conducted network pharmacology to explore the bioactive ingredients and related targets of WMW.

Results of 102 bioactive ingredients from the "herb-ingredient-target" network diagram and related topological parameters showed that the potential pivotal ingredients of WMW might be quercetin, candletoxin A, palmidin A, kaempferol, and beta-sitosterol. Quercetin and kaempferol may be the main anti-SDA active compounds, which are known as one of the families of flavonols and thought to be beneficial against cardiovascular diseases, cancer, diabetes, neurological diseases, obesity, allergy asthma, and atopic diseases with the effect of antioxidant, anti-inflammatory, cardioprotective, and anti-obesity.[47–49] Results from the epidemiological studies indicated that asthma incidence was lower at higher quercetin intakes (relative risk 0.76; 95% CI: 0.56, 1.01; P for trend= 0.005) and increased intake of kaempferol was associated with a low incidence of cerebrovascular disease.[50] Owing to the chronic airway inflammation of asthma, preventing oxidative damage and reducing inflammatory cytokines release of airways play a key role in the treatment of asthma. As previous studies reported, quercetin and kaempferol showed anti-allergic properties characterized by a decrease in Th2 related inflammatory cytokines (IL-4, IL-5, and IL-13), inhibition of histamine release and activation of mast cells (MCs), restrain antigen-specific IgE antibody formation, and elimination of the alterations in

Table 3 Relative Expression of IL-8 in All Groups

Group	Relative Expression of IL-8	Mean ± SEM
Control	0.102237757	0.14 ± 0.03
	0.113965311	
	0.203532817	
OVA	1.806670402	1.76 ± 0.30
	1.217003514	
	2.255321854	
OVA+DEX	1.543993487	1.16 ± 0.20
	0.903335201	
	1.025741121	
WMW	0.2258338	0.33 ± 0.19
	0.698984967	
	0.065304822	

cough reflex sensitivity.[51,52] Sitosterol is one of the bioactive phytosterols, which has shown the potential anti-inflammatory activity and antihistamine activity by inhibiting the release of histamine from the MCs, expression of TNF-α, and blocking the activity of cyclooxygenase-2, inducible nitric oxide synthase, and extracellular-signal regulating kinase pathways.[53] Moreover, it is proved that sitosterol treatment could significantly increase the tidal volume and decrease the respiration rate of asthmatic guinea pigs and protect against airway inflammation in lung tissue histopathology.[54] All in all, these studies about pivotal ingredients of WMW lend support to our findings of HUB gene GO and KEGG pathway enrichment analysis.

There were 35 HUB genes screened through the PPI network including *TP53, AKT1, MAPK1, JUN, HSP90AA1, TNF, RELA, IL6, CXCL8, EGFR*, etcetera. *TP53* is a tumor suppressor protein characterized by the regulation of glycolysis and oxidative phosphorylation, which is involved in several aspects of human function.[55] According to reports, the serum level of IL-1β was associated with *TP53* expression, and the high level of IL-1β might indicate the exacerbation of asthma due to airway epithelial apoptosis and injury.[56] *AKT1* regulates many cellular processes including metabolism, proliferation, cell survival, growth, and angiogenesis.[57] In the canine tracheal smooth muscle cell model, forced activation of AKT1 signaling will induce hypertrophy.[58] *RELA, IL6, CXCL8*, and *TNF* are all pro-inflammatory mediators, which participate in the chronic airway inflammation of SDA. As mentioned before, mixed neutrophilic/eosinophilic inflammation was more prevalent in SA patients, neutrophilic bronchitis leads to the overproduction of pro-inflammatory cytokines such as TNF, IL-1, IL-6, IL-8, IL-23, and IL-17.[59] As a multi-functional molecular chaperone, heat shock protein 90 (*HSP90*) is induced in response to cellular stress to stabilize client proteins, and the increased expression of *HSP90* is associated with asthma severity.[60] *HSP90* inhibitors could block the immune-mediated NF-κB inflammatory cascade and revert goblet cell metaplasia.[61,62] So maybe HSP90 inhibitors will be the next generation of biological agents. *EGFR* is expressed in airway epithelium and involved in the biological process of cell growth, proliferation, and differentiation.[63] PPI network analysis of gene expression profile of GSE7368 indicates that *EGFR* is associated with inflammatory environment and steroid resistance in asthma patients.[64] The impaired expression of *EGFR* is considered relevant to asthma pathogenesis in terms of airway inflammation, airway remodeling, airway hyper-responsiveness (AHR), and airway mucus secretion.[65] As a consequence of airway inflammation, epithelial damage and strong *EGFR* immunostaining are frequently observed in asthmatic patients.[66] Meanwhile, *EGFR* inhibitor treatment could reduce inflammatory cell influx in bronchoalveolar lavage fluid, perivascular and peribronchial inflammation, fibrosis, goblet cell hyper/metaplasia, and AHR in the OVA-induced animal model. *MAPK1* and *JUN* belong to the

MAPK family. MAPK pathways are involved in the activation of transcription factors such as NF-κB and AP-1, and the activation of p38 MAPK pathway could lead to glucocorticoid insensitivity for SA patients.[67–69] Furthermore, p38 MAPK is crucial in the allergic inflammatory cascade because it is needed in the upregulation of adhesion molecules on eosinophils and epithelial cells when allergy happens.[70] Another in-vitro experiment proves that the inhibition of p38 MAPK pathway may lead to additive and synergistic anti-inflammatory effects and reverse the glucocorticoid insensitivity when corticosteroids are used together.[71,72] Similarly, the 35 HUB genes screened through the PPI network in our study was in corroboration with the previous findings.

KEGG pathway enrichment analysis of HUB genes indicated that the IL-17 signaling pathway might be the potential mechanism of WMW against SDA. There have been a couple of studies suggesting that IL-17 plays a key role in the pathogenesis of SA.[73,74] SA might be related to the overexpression of Th 17 cytokines, which induce neutrophil recruitment via neutrophil-mobilizing cytokines in airways.[75] However, the mixed pattern of neutrophilic-eosinophilic infiltration in airways, and glucocorticoid insensitivity makes SA refractory to currently available therapies like ICS-LABA.[76] So what about biological agents? A randomized, double-blind, placebo-controlled study claimed that inhibition of IL-17 receptor A did not produce a treatment effect in subjects with moderate to SA.[77] Maybe the single targeted biological agents could not benefit SA patients with its complex pathogenesis and the monoclonal antibody therapy still has a long reach.

Given the active ingredients of WMW are complex, it is quite difficult to identify each ingredient by the traditional method. The improvement of molecular docking technology is promising in explaining the mechanism of TCM formulas. Molecular docking is a computational procedure that analyses the conformation and orientation of drug-protein into the binding site of a macromolecular target, which could discover the key pharmacodynamic components, reveal the pharmacodynamic material basis of the complex chemical substance system, and improve the efficiency and pertinence of the TCM screening process.[78] With the method of molecular docking, we could indirectly prove the interaction between molecules and exclude those connections with high degree scores but invalid ligand-receptor combinations from "herb-ingredient-target" network. Results from our study showed that potential pivotal ingredients of WMW had excellent abilities to spontaneously bind the receptor proteins of SDA. Meanwhile, CXCL8 had the lowest receptor protein-ligand interactions energy. As the gene expression production of CXCL8, IL-8 is regarded as a key mediator in neutrophil-mediated acute inflammation due to its potent actions on neutrophils.[79] It was reported that serum levels of IL-8 were significantly higher in patients with moderate asthma and SA as compared with healthy non-atopic controls, especially, higher IL-8 levels were associated with a pattern of current smokers.[80] Besides, several studies suggest that IL-17/Th 17 is involved in the process of IL-8 up-regulation,[81] which meets with our findings in KEGG pathway enrichment. Down-regulated expressions of IL-8 helps to reduce airway inflammation. In our study, the OVA group and OVA+DEX group showed obvious inflammatory cell infiltration and collagen deposition with high expression of IL-8 by IHC staining and real-time PCR, while WMW treatment reduced these pathological changes by inhibiting the secretion of IL-8. We couldn't confirm the specific bioactive ingredient in WMW which helps to down-regulate the IL-8 expression, but quercetin and kaempferol might be the main effecting ones. As reported by previous studies, quercetin and kaempferol could decrease the release of inflammatory mediators of TNF-α, IL-1β, IL-6, and IL-8 through inhibitions of the activation of IKKβ, blocks of the phosphorylation of IκBα, preventions of NF-KB entering into the nucleus, and the attenuation of NF-κB and p38 MAPK pathway, in which way inhibit the airway inflammation.[82,83] We will conduct more research around traditional Chinese medicine monomers to confirm our suppositions.

To better understand and elucidate the mechanisms of diseases, experimental animal models were widely used in the medical field. However, the experimental animal model of SDA is still at an initial and exploratory stage. Different from the classical allergic respiratory diseases animal model induced by OVA, consensuses on the methods of building the SDA animal models have not been achieved. Given allergic animal models require protocols of allergic sensitization and subsequent allergen re-exposure (challenge) to induce an allergic inflammatory response,[84] we built the OVA-induced plus descending DEX intervention chronic asthma model based on our previous study. On the one hand, this model, in common with classical allergic asthma models, satisfies the characteristics of allergic airway inflammation with two phases of OVA sensitization and inhaled challenge; on the other hand, descending DEX intervention simulates the descent use of glucocorticoid from a high-dose to a low-dose in the clinic, which might not be reflective in the classical

model. Results from H&E and Masson staining indicated OVA group rats and OVA+DEX group rats showed obvious airway inflammation and remodeling, which was consistent with pathology changes of SDA patients.[85] It`s quite strange to observe these obvious pathological changes in OVA+DEX group rats because DEX also has a strong anti-inflammation effect. While this might be related to over OCS uses induced neutrophil recruitments into airways and inhibitions of neutrophil apoptosis in airways, as previous reports suggested,[86] which explained the obvious inflammation and up-regulated expression of IL-8 in airways observed in the DEX group.

To our knowledge, this is the first study to discuss the effects of CHM on SDA. We wish more evidence of treating SDA with CHM will be reported in the future.

Conclusion

With the methods of network pharmacology and molecular docking, we conducted the "herb-ingredient-target" network of WMW. Five pivotal ingredients were obtained including quercetin, candletoxin A, palmidin A, kaempferol, and beta-sitosterol. Meanwhile, 35 HUB genes were screened out from the PPI network, namely, *TP53, AKT1, MAPK1, JUN, HSP90AA1, TNF, RELA, IL6, CXCL8, EGFR*, etcetera, which played key roles in the treatment of WMW against SDA and showed excellent abilities to spontaneously bind the pivotal ingredients in molecular docking. Based on the results of GO and KEGG pathway enrichment analysis, it was suggested that WMW treatment was effective against SDA by reducing inflammation with multi-pathways. In the experiment, we built the OVA-induced plus descending DEX intervention chronic asthmatic model and proved WMW treatment could reduce airway inflammation, airway remodeling, and the expression of IL-8 in model rats. In this paper, we claimed that WMW could be a complementary and alternative therapy for SDA.

Abbreviations

AHR, airway hyper-responsiveness; BATMAN-TCM, bioinformatics analysis tool for the molecular mechanism of traditional Chinese medicine database; BC, betweenness centrality; BPs, biological processes; CCs, cell components; CC, closeness centrality; CHM, Chinese herbal medicine; DAB, 3.3`-diaminobenzidine; DCs, degrees; DEX, dexamethasone sodium phosphate injection; DG, *Angelicae Sinensis Radix*; DL, drug likeness; FZ, *Aconiti Lateralis Radix Praeparata*; GINA, Global Initiative for Asthma; GJ, *Zingiberis Rhizoma*; GO, Gene Ontology; GR, glucocorticoid receptor; GZ, *Cinnamomi Ramulus*; HB, *Phellodendri Chinensis Cortex*; H&E, hematoxylin/eosin; HJ, *Zanthoxyli Pericarpium*; HL, *Coptidis Rhizoma*; HSP90, heat shock protein 90; ICS, inhaled corticosteroid; IHC, immunohistochemistry; KEGG, Kyoto Encyclopedia of Genes and Genomes; LABA, long-acting beta 2-agonist; MCs, mast cells; MFs, molecular functions; OB, oral bioavailability; OCS, oral corticosteroid; OMIM, Online Mendelian Inheritance in Man database; OVA, ovalbumin; PDB, RCSB Protein Data Bank database; PPI, protein-protein interaction; Real-time PCR, real-time quantitative polymerase chain reaction; RS, *Ginseng Radix Et Rhizoma*; SA, severe asthma; SDA, Steroid-dependent asthma; STRING, Search Tool for the Retrieval of Interacting Genes/Proteins; TCM, Traditional Chinese Medicine; TCMSP, traditional Chinese medicine systems pharmacology database; Th2, type 2 helper T; TTD, Therapeutic Target Database; UniProtKB, UniProt Knowledgebase; WM, *Mume Fructus*; WMW, Wumeiwan; XX, *Asari Radix Et Rhizoma.*

Acknowledgments

All authors would like to thank Dr. Wenchao Dan from Department of Cardiology, China Academy of Chinese Medical Sciences Guanganmen Hospital for his kindness help in the work of network pharmacology.

Disclosure

The authors report no conflicts of interest in this work.

References

1. Randhawa I, Klaustermeyer WB. Oral corticosteroid-dependent asthma: a 30-year review. *Ann Allergy Asthma Immunol*. 2007;99(4):291–302; quiz 302–303, 370. doi:10.1016/S1081-1206(10)60543-1
2. Pavord ID. Oral corticosteroid-dependent asthma: current knowledge and future needs. *Curr Opin Pulm Med*. 2019;25(1):51–58. doi:10.1097/MCP.0000000000000541

3. Rabe KF, Nair P, Brusselle G, et al. Efficacy and safety of dupilumab in glucocorticoid-dependent severe asthma. *N Engl J Med*. 2018;378(26):2475–2485. doi:10.1056/NEJMoa1804093
4. Bernstein JA, Virchow JC, Murphy K, et al. Effect of fixed-dose subcutaneous reslizumab on asthma exacerbations in patients with severe uncontrolled asthma and corticosteroid sparing in patients with oral corticosteroid-dependent asthma: results from two Phase 3, randomised, double-blind, placebo-controlled trials. *Lancet Respir Med*. 2020;8(5):461–474. doi:10.1016/S2213-2600(19)30372-8
5. Bleecker ER, Menzies-Gow AN, Price DB, et al. Systematic literature review of systemic corticosteroid use for asthma management. *Am J Respir Crit Care Med*. 2020;201(3):276–293. doi:10.1164/rccm.201904-0903SO
6. Volmer T, Effenberger T, Trautner C, Buhl R. Consequences of long-term oral corticosteroid therapy and its side-effects in severe asthma in adults: a focused review of the impact data in the literature. *Eur Respir J*. 2018;52(4):1800703. doi:10.1183/13993003.00703-2018
7. Janson C, Lisspers K, Stallberg B, et al. Health care resource utilization and cost for asthma patients regularly treated with oral corticosteroids - a Swedish observational cohort study (PACEHR). *Respir Res*. 2018;19(1):168. doi:10.1186/s12931-018-0855-3
8. Lyu MS, Li DY, Zhou SZ, Ban CJ, Yan J. Adult-onset still's disease successfully treated with Chinese herbal medicine: a case report with 15-month follow-up. *J Integr Med*. 2020;18(6):530–534. doi:10.1016/j.joim.2020.08.004
9. Wang W, Yao Q, Teng F, Cui J, Dong J, Wei Y. Active ingredients from Chinese medicine plants as therapeutic strategies for asthma: overview and challenges. *Biomed Pharmacother*. 2021;137:111383. doi:10.1016/j.biopha.2021.111383
10. Liao PF, Wang YT, Wang YH, Chiou JY, Wei JC. Traditional Chinese medicine use may reduce medical utility in patients with asthma: a nationwide population-based retrospective cohort study. *QJM*. 2021;114(12):857–864.
11. Cui HS, Fan HL, Wu WP. Therapeutic mechanism and clinical application of Wumeiwan in the treatment of steroid dependent asthma. *J Beijing Univ Trad Chin Med*. 2000;05:62–63.
12. Yang S, Wu WP, Cui HS. Analysis of Wumeiwan in the treatment of steroid dependent asthma. *Chin Arch Trad Chin Med*. 2005;03:438–439.
13. Cui HS, Wu WP, Ren CY. Clinical observation on 20 cases of steroid-dependent asthma treated with modified Wumeiwan. *J Basic Chin Med*. 2004;4(08):49–50.
14. Guo W, Huang J, Wang N, et al. Integrating network pharmacology and pharmacological evaluation for deciphering the action mechanism of herbal formula Zuojin pill in suppressing hepatocellular carcinoma. *Front Pharmacol*. 2019;10:1185. doi:10.3389/fphar.2019.01185
15. Zhang R, Zhu X, Bai H, Ning K. Network pharmacology databases for traditional Chinese medicine: review and assessment. *Front Pharmacol*. 2019;10:123. doi:10.3389/fphar.2019.00123
16. Wang X, Wang ZY, Zheng JH, Li S. TCM network pharmacology: a new trend towards combining computational, experimental and clinical approaches. *Chin J Nat Med*. 2021;19(1):1–11.
17. Societies WFoCM. Network pharmacology evaluation method guidance-draft. *World Chin Med*. 2021;16(04):527–532.
18. Ru J, Li P, Wang J, et al. TCMSP: a database of systems pharmacology for drug discovery from herbal medicines. *J Cheminform*. 2014;6:13. doi:10.1186/1758-2946-6-13
19. Liu Z, Guo F, Wang Y, et al. BATMAN-TCM: a bioinformatics analysis tool for molecular mechanism of traditional Chinese medicine. *Sci Rep*. 2016;6:21146. doi:10.1038/srep21146
20. Shi H, Dong C, Wang M, et al. Exploring the mechanism of Yizhi Tongmai decoction in the treatment of vascular dementia through network pharmacology and molecular docking. *Ann Transl Med*. 2021;9(2):164. doi:10.21037/atm-20-8165
21. Ye H, Ye L, Kang H, et al. HIT: linking herbal active ingredients to targets. *Nucleic Acids Res*. 2011;39(Databaseissue):D1055–1059. doi:10.1093/nar/gkq1165
22. Li X, Tang H, Tang Q, Chen W. Decoding the mechanism of Huanglian Jiedu decoction in treating pneumonia based on network pharmacology and molecular docking. *Front Cell Dev Biol*. 2021;9:638366. doi:10.3389/fcell.2021.638366
23. Stelzer G, Rosen N, Plaschkes I, et al. The GeneCards Suite: from gene data mining to disease genome sequence analyses. *Curr Protoc Bioinformatics*. 2016;54:1301–13033. doi:10.1002/cpbi.5
24. Amberger JS, Bocchini CA, Schiettecatte F, Scott AF, Hamosh A. OMIM.org: online Mendelian Inheritance in Man (OMIM(R)), an online catalog of human genes and genetic disorders. *Nucleic Acids Res*. 2015;43(Databaseissue):D789–798. doi:10.1093/nar/gku1205
25. Wang Y, Zhang S, Li F, et al. Therapeutic target database 2020: enriched resource for facilitating research and early development of targeted therapeutics. *Nucleic Acids Res*. 2020;48(D1):D1031–1031D1041. doi:10.1093/nar/gkz981
26. Pinero J, Ramirez-Anguita JM, Sauch-Pitarch J, et al. The DisGeNET knowledge platform for disease genomics: 2019 update. *Nucleic Acids Res*. 2020;48(D1):D845–845D855. doi:10.1093/nar/gkz1021
27. Shannon P, Markiel A, Ozier O, et al. Cytoscape: a software environment for integrated models of biomolecular interaction networks. *Genome Res*. 2003;13(11):2498–2504. doi:10.1101/gr.1239303
28. Szklarczyk D, Gable AL, Lyon D, et al. STRING v11: protein-protein association networks with increased coverage, supporting functional discovery in genome-wide experimental datasets. *Nucleic Acids Res*. 2019;47(D1):D607–607D613. doi:10.1093/nar/gky1131
29. Yu G, Zhang Y, Ren W, et al. Network pharmacology-based identification of key pharmacological pathways of Yin-Huang-Qing-Fei capsule acting on chronic bronchitis. *Int J Chron Obstruct Pulmon Dis*. 2017;12:85–94. doi:10.2147/COPD.S121079
30. Zhou Y, Zhou B, Pache L, et al. Metascape provides a biologist-oriented resource for the analysis of systems-level datasets. *Nat Commun*. 2019;10(1):1523. doi:10.1038/s41467-019-09234-6
31. Morris GM, Huey R, Lindstrom W, et al. AutoDock4 and AutoDockTools4: automated docking with selective receptor flexibility. *J Comput Chem*. 2009;30(16):2785–2791. doi:10.1002/jcc.21256
32. Burley SK, Bhikadiya C, Bi C, et al. RCSB Protein Data Bank: powerful new tools for exploring 3D structures of biological macromolecules for basic and applied research and education in fundamental biology, biomedicine, biotechnology, bioengineering and energy sciences. *Nucleic Acids Res*. 2021;49(D1):D437–437D451. doi:10.1093/nar/gkaa1038
33. Qin F, Cheng J, Cui H, et al.Three-step sequential therapy on pathomorphology of bronchial lung tissues of asthmatic rat airway remodeling after hormone intervention. *J Beijing Univ Trad Chin Med*. 2016;39(08):670–678.
34. Liu Y, Pu Y, Li D, Zhou L, Wan L. Azithromycin ameliorates airway remodeling via inhibiting airway epithelium apoptosis. *Life Sci*. 2017;170:1–8. doi:10.1016/j.lfs.2016.11.024
35. Zhao H, Gao XY, Wu XJ, Zhang YB, Wang XF. The Shh/Gli1 signaling pathway regulates regeneration via transcription factor Olig1 expression after focal cerebral ischemia in rats. *Neurol Res*. 2021;1–13. doi:10.1080/01616412.2021.1981106

36. Bardou P, Mariette J, Escudie F, Djemiel C, Klopp C. jvenn: an interactive Venn diagram viewer. *BMC Bioinform*. 2014;15:293. doi:10.1186/1471-2105-15-293
37. Li C, Du X, Liu Y, et al. A systems pharmacology approach for identifying the multiple mechanisms of action for the Rougui-Fuzi herb pair in the treatment of cardiocerebral vascular diseases. *Evid Based Complement Alternat Med*. 2020;2020:5196302. doi:10.1155/2020/5196302
38. Heaney LG, Brightling CE, Menzies-Gow A, Stevenson M, Niven RM; British Thoracic Society Difficult Asthma N. Refractory asthma in the UK: cross-sectional findings from a UK multicentre registry. *Thorax*. 2010;65(9):787–794. doi:10.1136/thx.2010.137414
39. Hammad H, Lambrecht BN. The basic immunology of asthma. *Cell*. 2021;184(9):2521–2522. doi:10.1016/j.cell.2021.04.019
40. Yılmaz İ. Biologics for oral corticosteroid-dependent asthma. *Allergy Asthma Proc*. 2020;41(3):151–157. doi:10.2500/aap.2020.41.200015
41. Rossios C, Pavlidis S, Hoda U, et al. Sputum transcriptomics reveal upregulation of IL-1 receptor family members in patients with severe asthma. *J Allergy Clin Immunol*. 2018;141(2):560–570. doi:10.1016/j.jaci.2017.02.045
42. Fan H, Qiu MY, Mei JJ, Shen GX, Liu SL, Chen R. Effects of four regulating-intestine prescriptions on pathology and ultrastructure of colon tissue in rats with ulcerative colitis. *World J Gastroenterol*. 2005;11(31):4800–4806. doi:10.3748/wjg.v11.i31.4800
43. Yang X, Lu F, Li L, et al. Wu-Mei-wan protects pancreatic beta cells by inhibiting NLRP3 inflammasome activation in diabetic mice. *BMC Complement Altern Med*. 2019;19(1):35. doi:10.1186/s12906-019-2443-6
44. Wu F, Shao Q, Hu M, et al. Wu-Mei-Wan ameliorates chronic colitis-associated intestinal fibrosis through inhibiting fibroblast activation. *J Ethnopharmacol*. 2020;252:112580. doi:10.1016/j.jep.2020.112580
45. Wu F, Yang X, Hu M, et al. Wu-Mei-Wan prevents high-fat diet-induced obesity by reducing white adipose tissue and enhancing brown adipose tissue function. *Phytomedicine*. 2020;76:153258. doi:10.1016/j.phymed.2020.153258
46. Wang J, Jones SM, Pongracic JA, et al. Safety, clinical, and immunologic efficacy of a Chinese herbal medicine (Food Allergy Herbal Formula-2) for food allergy. *J Allergy Clin Immunol*. 2015;136(4):962–970 e1. doi:10.1016/j.jaci.2015.04.029
47. Duan L, Ding W, Liu X, et al. Biosynthesis and engineering of kaempferol in Saccharomyces cerevisiae. *Microb Cell Fact*. 2017;16(1):165. doi:10.1186/s12934-017-0774-x
48. Imran M, Rauf A, Shah ZA, et al. Chemo-preventive and therapeutic effect of the dietary flavonoid kaempferol: a comprehensive review. *Phytother Res*. 2019;33(2):263–275. doi:10.1002/ptr.6227
49. Ulusoy HG, Sanlier N. A minireview of quercetin: from its metabolism to possible mechanisms of its biological activities. *Crit Rev Food Sci Nutr*. 2020;60(19):3290–3303. doi:10.1080/10408398.2019.1683810
50. Knekt P, Kumpulainen J, Jarvinen R, et al. Flavonoid intake and risk of chronic diseases. *Am J Clin Nutr*. 2002;76(3):560–568. doi:10.1093/ajcn/76.3.560
51. Mlcek J, Jurikova T, Skrovankova S, Sochor J. Quercetin and its anti-allergic immune response. *Molecules*. 2016;21(5):623. doi:10.3390/molecules21050623
52. Molitorisova M, Sutovska M, Kazimierova I, et al. The anti-asthmatic potential of flavonol kaempferol in an experimental model of allergic airway inflammation. *Eur J Pharmacol*. 2021;891:173698. doi:10.1016/j.ejphar.2020.173698
53. Marahatha R, Gyawali K, Sharma K, et al. Pharmacologic activities of phytosteroids in inflammatory diseases: mechanism of action and therapeutic potentials. *Phytother Res*. 2021;35(9):5103–5124. doi:10.1002/ptr.7138
54. Mahajan SG, Mehta AA. Suppression of ovalbumin-induced Th2-driven airway inflammation by beta-sitosterol in a Guinea pig model of asthma. *Eur J Pharmacol*. 2011;650(1):458–464. doi:10.1016/j.ejphar.2010.09.075
55. Puzio-Kuter AM. The role of p53 in metabolic regulation. *Genes Cancer*. 2011;2(4):385–391. doi:10.1177/1947601911409738
56. Uddin MA, Barabutis N. P53 in the impaired lungs. *DNA Repair (Amst)*. 2020;95:102952. doi:10.1016/j.dnarep.2020.102952
57. Hers I, Vincent EE, Tavare JM. Akt signalling in health and disease. *Cell Signal*. 2011;23(10):1515–1527. doi:10.1016/j.cellsig.2011.05.004
58. Ma L, Brown M, Kogut P, et al. Akt activation induces hypertrophy without contractile phenotypic maturation in airway smooth muscle. *Am J Physiol Lung Cell Mol Physiol*. 2011;300(5):L701–709. doi:10.1152/ajplung.00119.2009
59. Svenningsen S, Nair P. Asthma endotypes and an overview of targeted therapy for asthma. *Front Med (Lausanne)*. 2017;4:158. doi:10.3389/fmed.2017.00158
60. Lee MY, Sun KH, Chiang CP, et al. Nitric oxide suppresses LPS-induced inflammation in a mouse asthma model by attenuating the interaction of IKK and Hsp90. *Exp Biol Med (Maywood)*. 2015;240(4):498–507. doi:10.1177/1535370214554880
61. Shimp SK, Parson CD, Regna NL, et al. HSP90 inhibition by 17-DMAG reduces inflammation in J774 macrophages through suppression of Akt and nuclear factor-kappaB pathways. *Inflamm Res*. 2012;61(5):521–533. doi:10.1007/s00011-012-0442-x
62. Pezzulo AA, Tudas RA, Stewart CG, et al. HSP90 inhibitor geldanamycin reverts IL-13- and IL-17-induced airway goblet cell metaplasia. *J Clin Invest*. 2019;129(2):744–758. doi:10.1172/JCI123524
63. Inoue H, Akimoto K, Homma T, Tanaka A, Sagara H. Airway epithelial dysfunction in asthma: relevant to epidermal growth factor receptors and airway epithelial cells. *J Clin Med*. 2020;9(11):3698. doi:10.3390/jcm9113698
64. Vargas JE, Porto BN, Puga R, Stein RT, Pitrez PM. Identifying a biomarker network for corticosteroid resistance in asthma from bronchoalveolar lavage samples. *Mol Biol Rep*. 2016;43(7):697–710. doi:10.1007/s11033-016-4007-x
65. Puddicombe SM, Polosa R, Richter A, et al. Involvement of the epidermal growth factor receptor in epithelial repair in asthma. *FASEB J*. 2000;14(10):1362–1374. doi:10.1096/fasebj.14.10.1362
66. El-Hashim AZ, Khajah MA, Renno WM, et al. Src-dependent EGFR transactivation regulates lung inflammation via downstream signaling involving ERK1/2, PI3Kdelta/Akt and NFkappaB induction in a murine asthma model. *Sci Rep*. 2017;7(1):9919. doi:10.1038/s41598-017-09349-0
67. Bhavsar P, Hew M, Khorasani N, et al. Relative corticosteroid insensitivity of alveolar macrophages in severe asthma compared with non-severe asthma. *Thorax*. 2008;63(9):784–790. doi:10.1136/thx.2007.090027
68. Li LB, Leung DY, Goleva E. Activated p38 MAPK in peripheral blood monocytes of steroid resistant asthmatics. *PLoS One*. 2015;10(10):e0141909. doi:10.1371/journal.pone.0141909
69. Marwick JA, Tudor C, Khorasani N, Michaeloudes C, Bhavsar PK, Chung KF. Oxidants induce a corticosteroid-insensitive phosphorylation of histone 3 at serine 10 in monocytes. *PLoS One*. 2015;10(4):e0124961. doi:10.1371/journal.pone.0124961
70. Chung KF. p38 mitogen-activated protein kinase pathways in asthma and COPD. *Chest*. 2011;139(6):1470–1479. doi:10.1378/chest.10-1914
71. Bhavsar P, Khorasani N, Hew M, Johnson M, Chung KF. Effect of p38 MAPK inhibition on corticosteroid suppression of cytokine release in severe asthma. *Eur Respir J*. 2010;35(4):750–756. doi:10.1183/09031936.00071309

72. Lea S, Li J, Plumb J, et al. P38 MAPK and glucocorticoid receptor crosstalk in bronchial epithelial cells. *J Mol Med (Berl)*. 2020;98(3):361–374. doi:10.1007/s00109-020-01873-3
73. Chesne J, Braza F, Mahay G, Brouard S, Aronica M, Magnan A. IL-17 in severe asthma. Where do we stand? *Am J Respir Crit Care Med*. 2014;190(10):1094–1101. doi:10.1164/rccm.201405-0859PP
74. Linden A, Dahlen B. Interleukin-17 cytokine signalling in patients with asthma. *Eur Respir J*. 2014;44(5):1319–1331. doi:10.1183/09031936.00002314
75. Ricciardolo FLM, Sorbello V, Folino A, et al. Identification of IL-17F/frequent exacerbator endotype in asthma. *J Allergy Clin Immunol*. 2017;140(2):395–406. doi:10.1016/j.jaci.2016.10.034
76. Ramakrishnan RK, Al Heialy S, Hamid Q. Role of IL-17 in asthma pathogenesis and its implications for the clinic. *Expert Rev Respir Med*. 2019;13(11):1057–1068. doi:10.1080/17476348.2019.1666002
77. Busse WW, Holgate S, Kerwin E, et al. Randomized, double-blind, placebo-controlled study of brodalumab, a human anti-IL-17 receptor monoclonal antibody, in moderate to severe asthma. *Am J Respir Crit Care Med*. 2013;188(11):1294–1302. doi:10.1164/rccm.201212-2318OC
78. Jiao X, Jin X, Ma Y, et al. A comprehensive application: molecular docking and network pharmacology for the prediction of bioactive constituents and elucidation of mechanisms of action in component-based Chinese medicine. *Comput Biol Chem*. 2021;90:107402. doi:10.1016/j.compbiolchem.2020.107402
79. Mukaida N. Pathophysiological roles of interleukin-8/CXCL8 in pulmonary diseases. *Am J Physiol Lung Cell Mol Physiol*. 2003;284(4):L566–577. doi:10.1152/ajplung.00233.2002
80. Dimitrova D, Youroukova V, Ivanova-Todorova E, Tumangelova-Yuzeir K, Velikova T. Serum levels of IL-5, IL-6, IL-8, IL-13 and IL-17A in pre-defined groups of adult patients with moderate and severe bronchial asthma. *Respir Med*. 2019;154:144–154. doi:10.1016/j.rmed.2019.06.024
81. Nakagome K, Matsushita S, Nagata M. Neutrophilic inflammation in severe asthma. *Int Arch Allergy Immunol*. 2012;158(Suppl 1):96–102. doi:10.1159/000337801
82. Min YD, Choi CH, Bark H, et al. Quercetin inhibits expression of inflammatory cytokines through attenuation of NF-kappaB and p38 MAPK in HMC-1 human mast cell line. *Inflamm Res*. 2007;56(5):210–215. doi:10.1007/s00011-007-6172-9
83. Zhou YJ, Wang H, Li L, Sui HH, Huang JJ. Inhibitory effect of kaempferol on inflammatory response of lipopolysaccharide-stimulated human mast cells. *Yao Xue Xue Bao*. 2015;50(6):702–707.
84. Paiva Ferreira LKD, Paiva Ferreira LAM, Monteiro TM, Bezerra GC, Bernardo LR, Piuvezam MR. Combined allergic rhinitis and asthma syndrome (CARAS). *Int Immunopharmacol*. 2019;74:105718. doi:10.1016/j.intimp.2019.105718
85. Jeffery PK. Remodeling in asthma and chronic obstructive lung disease. *Am J Respir Crit Care Med*. 2001;164(10 Pt 2):S28–38. doi:10.1164/ajrccm.164.supplement_2.2106061
86. Nguyen LT, Lim S, Oates T, Chung KF. Increase in airway neutrophils after oral but not inhaled corticosteroid therapy in mild asthma. *Respir Med*. 2005;99(2):200–207. doi:10.1016/j.rmed.2004.06.007